



PII S0016-7037(02)01039-6

Self-diffusion of Si and O in diopside-anorthite melt at high pressures

DAVID TINKER,^{1,*} CHARLES E. LESHER,¹ and IAN D. HUTCHEON²¹Department of Geology, University of California, One Shields Ave., Davis, CA 95616, USA²Analytical & Nuclear Chemistry Division, Lawrence Livermore National Laboratory, P.O. Box 808, Livermore, CA 94551-0808, USA

(Received May 15, 2001; accepted in revised form June 24, 2002)

Abstract—Self-diffusion coefficients for Si and O in $\text{Di}_{58}\text{An}_{42}$ liquid were measured from 1 to 4 GPa and temperatures from 1510 to 1764°C. Glass starting powders enriched in ^{18}O and ^{28}Si were mated to isotopically normal glass powders to form simple diffusion couples, and self-diffusion experiments were conducted in the piston cylinder device (1 and 2 GPa) and in the multianvil apparatus (3.5 and 4 GPa). Profiles of $^{18}\text{O}/^{16}\text{O}$ and $^{29,30}\text{Si}/^{28}\text{Si}$ were measured using secondary ion mass spectrometry. Self-diffusion coefficients for O ($D(\text{O})$) are slightly greater than self-diffusion coefficients for Si ($D(\text{Si})$) and are often the same within error. For example, $D(\text{O}) = 4.20 \pm 0.42 \times 10^{-11} \text{ m}^2/\text{s}$ and $D(\text{Si}) = 3.65 \pm 0.37 \times 10^{-11} \text{ m}^2/\text{s}$ at 1 GPa and 1662°C. Activation energies for self-diffusion are $215 \pm 13 \text{ kJ/mol}$ for O and $227 \pm 13 \text{ kJ/mol}$ for Si. Activation volumes for self-diffusion are $-2.1 \pm 0.4 \text{ cm}^3/\text{mol}$ and $-2.3 \pm 0.4 \text{ cm}^3/\text{mol}$ for O and Si, respectively. The similar self-diffusion coefficients for Si and O, similar activation energies, and small, negative activation volumes are consistent with Si and O transport by a cooperative diffusion mechanism, most likely involving the formation and disassociation of a high-coordinated intermediate species. The small absolute magnitudes of the activation volumes imply that $\text{Di}_{58}\text{An}_{42}$ liquid is close to a transition from negative to positive activation volume, and Adam-Gibbs theory suggests that this transition is linked to the existence of a critical fraction (~ 0.6) of bridging oxygen. Copyright © 2003 Elsevier Science Ltd

1. INTRODUCTION

Self-diffusion and viscous flow properties of silicate liquids are determined by the bonding environments of silicon (Si) and oxygen (O). The transport of Si and O depends on pressure, and a number of experimental studies (e.g., Shimizu and Kushiro, 1984; Poe et al., 1997; Tinker and Lesher, 2001), molecular dynamics (MD) simulations (e.g., Nevins and Spera, 1998; Bryce et al., 1999), and nuclear magnetic resonance (NMR) studies (e.g., Liu et al., 1988; Stebbins and McMillan, 1989) have focused on the link between the transported species and liquid structure at high pressures.

Shimizu and Kushiro (1984) studied O self-diffusion in jadeite melt and diopside melt and reported that O self-diffusion coefficients increased with pressure from 0.5 to 2 GPa in polymerized jadeite melt and decreased with pressure from 1 to 1.7 GPa in depolymerized diopside melt. The positive pressure dependence for O self-diffusion in jadeite melt corresponds to a negative activation volume, which Shimizu and Kushiro (1984) interpreted as reflecting a collapse of the melt structure. In contrast, the negative pressure dependence for O self-diffusion in diopside corresponds to a positive activation volume, and Shimizu and Kushiro (1984) interpreted this as reflecting expansion of the melt structure. In a more recent study, Shimizu and Kushiro (1991) studied Si self-diffusion in compositions along the diopside-jadeite join and found a transition from positive to negative pressure dependence of self-diffusion near $\text{Di}_{30}\text{Jd}_{70}$ (mol.%) (Fig. 1). A corollary of this result is the fact that the activation volume for Si self-diffusion is vanishingly small for $\text{Di}_{30}\text{Jd}_{70}$ liquid at 1 GPa.

The data summarized in Figure 1 show that changes in liquid

structure (e.g., NBO/T) are accompanied by changes in activation volume controlling self-diffusion. These structural changes may be analogous to changes in structure occurring during compression of a single liquid composition. In some polymerized liquid compositions, self-diffusion coefficients increase on initial compression, reach maximum values, and then decrease with increasing pressure. Activation volumes in these liquids go from negative to positive, similar to the activation volumes calculated for decreasingly polymerized liquids in the Di-Jd system. Tinker and Lesher (2001) reported experimental results showing that both Si and O self-diffusion coefficients have maxima at roughly 5 GPa in dacitic liquid. Similarly, Poe et al. (1997) observed maximum self-diffusion coefficients for O in albite (at 5 GPa) and $\text{Na}_3\text{AlSi}_7\text{O}_{17}$ (at 8 GPa) liquids. Maximum self-diffusion coefficients near 30 GPa were predicted in early MD simulations for O self-diffusion in jadeite liquid (Angell et al., 1982). More recently, Nevins and Spera (1998) predicted maximum self-diffusion coefficients for Si and O near 5 GPa in a MD simulation study of anorthite ($\text{CaAl}_2\text{Si}_2\text{O}_8$) liquid, and Bryce et al. (1999) predicted maximum self-diffusion coefficients for Si, Al, and O at 21 GPa in nepheline, jadeite, and albite liquids at 5000 K. Conversely, in depolymerized compositions, self-diffusion coefficients for O can reach minimum values with increasing pressure. Reid et al. (2001) conducted an experimental study of Si and O self-diffusion in diopside liquid between 3 and 15 GPa and reported minimum self-diffusion coefficients for both Si and O at 11 GPa.

The goal of the present study is to improve our understanding of the transition from negative to positive activation volume. There are no previous experimental studies of O self-diffusion in intermediate compositions along compositional joins, so we have chosen to measure Si and O self-diffusion coefficients in the 1 atm eutectic composition 58 wt.% diop-

* Author to whom correspondence should be addressed (Tinker@geology.ucdavis.edu).

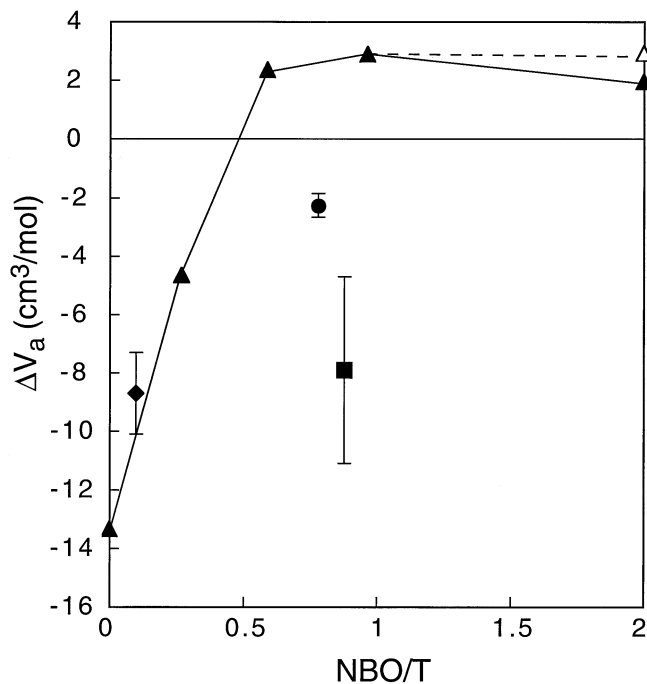


Fig. 1. Variation of activation volume (ordinate) for Si self-diffusion with changes in the degree of polymerization of liquids (abscissa). The degree of polymerization is measured as the ratio of nonbridging oxygen to tetrahedral cation (NBO/T). Fully polymerized liquids have NBO/T = 0 and completely depolymerized liquids have NBO/T = 4 (e.g., Mysen, 1990). Activation volumes for Si self-diffusion in Di-Jd liquid compositions at 1550°C (filled triangles) decrease with increasing polymerization from endmember Di to Jd, and there is a transition from positive to negative activation volume at NBO/T = 0.445 (Shimizu and Kushiro, 1991). Data from Shimizu and Kushiro (1991) are used to calculate the activation volumes for Si in Di (NBO/T = 2) (2 cm³/mol), in Di₆₀Jd₄₀ (mol.%, NBO/T = 0.97) (2.9 cm³/mol), in Di₄₀Jd₆₀ (NBO/T = 0.59) (2.35 cm³/mol), in Di₂₀Jd₈₀ (NBO/T = 0.27) (-4.7 cm³/mol), and in Jd (NBO/T = 0) (-13.4 cm³/mol). An alternative activation volume for Si self-diffusion in Di (3 cm³/mol, open triangle) is calculated using data from Reid et al. (2001). For comparison, the activation volume for Si in dacitic liquid (diamond) is -8.7 cm³/mol at 1561°C, and the activation volume for Si in basaltic liquid (square) is -7.9 cm³/mol from 1 to 2 GPa between 1320 and 1600°C (Lesher et al., 1996; Tinker and Lesher, 2001). The activation volume for Si self-diffusion in Di₅₈An₄₂ liquid (NBO/T = 0.8) (filled circle) is -2.3 cm³/mol. Interpolation between Di₅₈An₄₂ and Di suggests that the transition from positive to negative activation volume on the Di-An join occurs when NBO/T is between 1.2 and 1.4.

side-42 wt.% anorthite (64 mol.% Di-36 mol.% An) liquid (Di₅₈An₄₂). The Di-An system is a good, simple analog for naturally occurring basalts and the viscosity (Scarfe et al., 1983), and O self-diffusion coefficients (Dunn, 1982) have been measured in Di-An liquids at atmospheric pressure.

Here we report the results of laboratory measurements of the simultaneous self-diffusion of Si and O in Di₅₈An₄₂ liquid from 1 to 4 GPa between 1510 and 1764°C. The new results of this study suggest that this liquid is near a compositional transition from positive to negative pressure dependence. The self-diffusion of Si and O in Di₅₈An₄₂ liquid probably occurs through the formation of a high-coordinated intermediate species. We evaluate our results using a configurational entropy model for viscosity (Adam and Gibbs, 1965) and suggest that the pressure

Table 1. Starting compositions of the isotopically enriched and normal diopside-anorthite compositions measured using the Cameca SX-50 electron microprobe at UC Davis.

	"Enriched"	"Normal"
SiO ₂	50.14	49.54
Al ₂ O ₃	17.81	17.67
MgO	9.87	9.62
CaO	23.91	23.43

Chemical reagents from Fisher Scientific.
¹⁸O-enriched CO₂ and ²⁸Si-enriched SiO₂ from Cambridge Isotope Lab.

dependence of Si and O self-diffusion depends on a critical fraction of nonbridging O in the liquid.

2. EXPERIMENTAL PROCEDURES

Starting materials (Table 1) were synthesized from laboratory reagents following the methods described by Tinker and Lesher (2001). Self-diffusion experiments were conducted at 1, 2, 3.5, and 4 GPa and between 1510 and 1764°C. Experiments at 1 and 2 GPa were performed in a 0.5-inch Boyd and England piston cylinder apparatus (Boyd and England, 1960), and the experiments at 3.5 and 4 GPa were performed in a Walker 6/8 multi-anvil device (Walker et al., 1990). The configuration of the experimental assembly, a description of pressure and temperature calibration of the experimental apparatus, and details of the experimental procedure are available in Tinker and Lesher (2001).

Silicon and oxygen isotope gradients were measured using a modified Cameca IMS 3f ion microprobe at Lawrence Livermore National Laboratory. We used a primary ion beam of ¹⁶O⁻ accelerated to 12.5 or 15 KeV. The beam current was ~2 nA, and the beam was focused to yield a spot size of ≤ 20 μm. Negative secondary ions were accelerated to a nominal energy of 4500 eV and focused into the mass spectrometer operated at a mass resolving power of ~2800. This resolving power was sufficient to ensure ²⁸SiH⁻ contributed < 0.2% of the ²⁹Si⁻ intensity; ¹⁶OH₂⁻ is fully separated from ¹⁸O⁻ at this mass resolving power. The accelerating potential was offset by -30V (to 4470V) before each measurement of ¹⁶O⁻ to reduce the intensity below 1 × 10⁶ per second. Data were collected by stepping the magnet through the mass sequence 15.8, 16 (O), 18 (O), 28 (Si), 29 (Si), and 30 (Si) amu. Count times were 1 s for ¹⁶O, ¹⁸O, and ²⁸Si; 3 s for ²⁹Si; and 4 s for ³⁰Si. Secondary ion intensities were measured by pulse counting. Typical intensities (per second) for ²⁸Si, ²⁹Si, ³⁰Si, ¹⁶O, and ¹⁸O in the isotopically normal Di₅₈An₄₂ composition were 30,000, 1500, 1000, 700,000, and 2000, respectively. In the isotopically enriched endmember composition, intensities (per second) for ²⁸Si, ²⁹Si, ³⁰Si, ¹⁶O, and ¹⁸O were 35,000, 1000, 650, 700,000, and 15,000, respectively. Diffusion profiles were calculated by determining the changes in O and Si isotope compositions as a function of position along traverses across the diffusion interface. Traverses typically consisted of 20 points, with a 50- to 60-μm step size. The precision of isotope ratio measurements for each analysis was usually within a factor of 1.5 of the limit imposed by counting statistics and was typically ~0.4 to 0.5%.

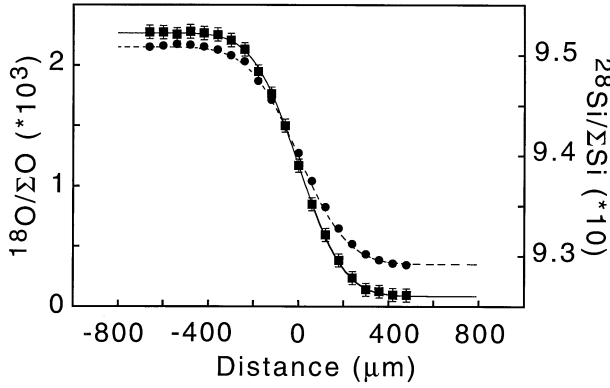


Fig. 2. Isotopic profiles for ^{28}Si ($^{28}\text{Si}/\Sigma\text{Si}$, squares) and ^{18}O ($^{18}\text{O}/\Sigma\text{O}$, circles) for a sample run at 3.5 GPa and 1662°C for 300 s. Isotopic abundances were measured using the Cameca 3f ion microprobe at the Lawrence Livermore National Laboratory. The distance (z) along the horizontal axis is in μm relative to the isotopically normal reservoir-enriched reservoir interface (the inflection point of the profile is taken to be $z = 0$). Curves through data are model isotope profiles generated using calculated diffusion coefficients ($5.00 \times 10^{-11} \text{ m}^2/\text{s}$ for O and $4.25 \times 10^{-11} \text{ m}^2/\text{s}$ for Si) in Fick's second law.

No corrections for instrumental mass-dependent isotope fractionation were applied.

3. RESULTS

Examples of isotopic abundance profiles are shown in Figure 2, where measured profiles for ^{28}Si and ^{18}O are compared to profiles calculated using Fick's second law, with the self-diffusion coefficients reported in Table 2. The self-diffusion profiles are monotonic and asymptotically approach the starting compositions for the normal and enriched endmembers. Figure 2 also shows that the width of the diffusion zone for ^{18}O is comparable to the width of the diffusion zone for ^{28}Si , suggesting that $D(\text{O}) \approx D(\text{Si})$.

Self-diffusion coefficients (D) were calculated using the solution for diffusion in a semi-infinite medium (Crank, 1975):

$$C = \frac{C1 + C2}{2} + \frac{C1 - C2}{2} \left(\text{erf} \frac{|z|}{2\sqrt{Dt}} \right) \quad (1)$$

where $C1$ and $C2$ are the isotope abundances for ^{28}Si or ^{18}O in

the enriched and normal starting materials, and C is the measured isotope abundance at a distance z from the normal-enriched interface at time t . The inflection of the isotopic profile is taken as the diffusion interface and is treated here as $z = 0$. The values for D were derived from the slopes of least squares best fit lines to plots of y vs. z , where

$$y \equiv \text{erf}^{-1} \left(\frac{2C - (C1 + C2)}{C1 - C2} \right) = \frac{|z|}{2\sqrt{Dt}} \quad (2)$$

is the inverted solution to the diffusion equation, as described by Shimizu and Kushiro (1984). The linearized solution to the diffusion Eqn. 2 gives an isotopic gradient across the normal-enriched interface whose slope is used to calculate the diffusion coefficient (Shimizu and Kushiro, 1984).

Diffusion coefficients for Si and O are reported with an error of 10%, determined by the reproducibility of multiple transects with the ion microprobe. Errors on reported isotopic abundances at individual points represent the standard deviation of the mean for 20 measurements of each ratio. In addition to analytical errors, uncertainties in reported diffusion coefficients may be introduced by deformation of the experimental charge. Specifically, thermal expansion and isothermal compressibility during quenching and decompression of an experimental charge can affect the length of a diffusion profile. We estimate these effects for our experimental conditions following Tinker and Leshner (2001), using partial molar volume data for oxide melt components from Lange (1997). The most extreme deformation of the diffusion couple likely in the experimental conditions of this study will lead to an overestimate of the self-diffusion coefficient by 6%, which is less than our reported uncertainty.

Figures 3 and 4 are plots of the temperature and pressure dependence of Si and O self-diffusion coefficients in $\text{Di}_{58}\text{An}_{42}$ liquid. Figure 3a shows the increases in natural logarithms of the self-diffusion coefficients for O ($\ln D(\text{O})$) with increasing temperature, and Figure 3b shows the increases in natural logarithms of the self-diffusion coefficients for Si ($\ln D(\text{Si})$) with increasing temperature. Figures 4a and 4b illustrate the increases in $\ln D(\text{O})$ and $\ln D(\text{Si})$ values, respectively, with increasing pressure.

Multiple linear regressions on D , P/T , and $1/T$ for the self-diffusion data collected in this study were used to determine the

Table 2. Run conditions and calculated self-diffusion coefficients for Si and O in $\text{Di}_{58}\text{An}_{42}$ liquid.

P (GPa)	Run duration (sec)	T (°C)	D(O) (m^2/s)	D(Si) (m^2/s)
1	900	1510	$1.25 \pm 0.13 \times 10^{-11}$	$8.00 \pm 0.80 \times 10^{-12}$
1	900	1561	$1.50 \pm 0.15 \times 10^{-11}$	$1.40 \pm 0.14 \times 10^{-11}$
1	600	1612	$2.65 \pm 0.27 \times 10^{-11}$	$2.20 \pm 0.22 \times 10^{-11}$
1	900	1662	$4.20 \pm 0.42 \times 10^{-11}$	$3.65 \pm 0.37 \times 10^{-11}$
1	600	1713	$5.00 \pm 0.50 \times 10^{-11}$	$3.33 \pm 0.33 \times 10^{-11}$
2	300	1612	$3.33 \pm 0.33 \times 10^{-11}$	$2.49 \pm 0.25 \times 10^{-11}$
2	900	1662	$4.50 \pm 0.45 \times 10^{-11}$	$3.70 \pm 0.37 \times 10^{-11}$
2	180	1713	$6.05 \pm 0.61 \times 10^{-11}$	$4.88 \pm 0.49 \times 10^{-11}$
3.5	935	1662	$4.85 \pm 0.49 \times 10^{-11}$	$3.75 \pm 0.38 \times 10^{-11}$
3.5	300	1662	$5.00 \pm 0.50 \times 10^{-11}$	$4.25 \pm 0.43 \times 10^{-11}$
3.5	180	1713	$7.40 \pm 0.74 \times 10^{-11}$	$6.50 \pm 0.65 \times 10^{-11}$
3.5	180	1764	$8.75 \pm 0.88 \times 10^{-11}$	$7.25 \pm 0.73 \times 10^{-11}$
4	240	1662	$5.10 \pm 0.51 \times 10^{-11}$	$4.50 \pm 0.45 \times 10^{-11}$
4	150	1713	$9.00 \pm 0.90 \times 10^{-11}$	$7.23 \pm 0.72 \times 10^{-11}$

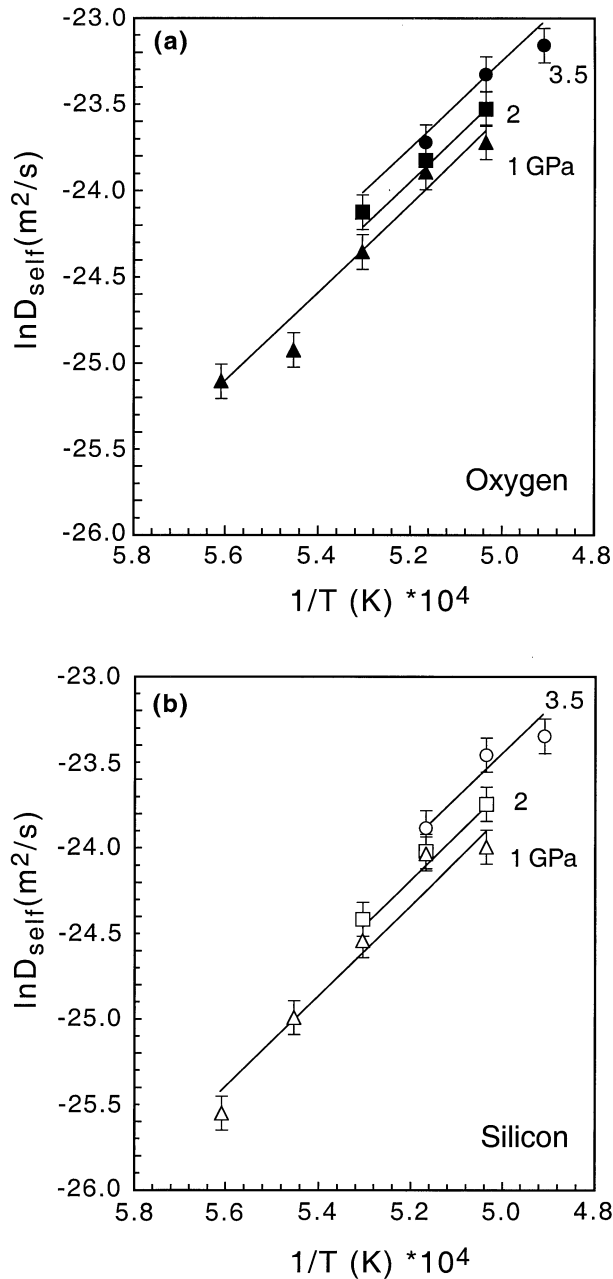


Fig. 3. (a) Variation of $\ln D(O)$ with reciprocal temperature. Data are plotted with 10% error bars on $D(O)$, determined by the reproducibility of multiple transects with the ion microprobe. The lines through these data are generated using the Arrhenius relationship $\ln D = \ln D_0 - (E_a + P\Delta V_a)/RT$. Multiple linear regression gives $E_a = 215 \pm 13$ kJ/mol for O self-diffusion. (b) Variation of $\ln D(Si)$ with reciprocal temperature. As in (a), data are plotted with 10% errors on $D(Si)$. The lines through these data are generated using the Arrhenius relationship used for (a). Multiple linear regression gives $E_a = 227 \pm 13$ kJ/mol for Si self-diffusion.

coefficients in the relationship $\ln D = \ln D_0 - (E_a + P\Delta V_a)/RT$, where D is the self-diffusion coefficient, D_0 is the preexponential factor, E_a is the activation energy, ΔV_a is the activation volume, R is the gas constant, and T is the temperature in Kelvin. The relationship for O is $\ln D = -10.8 \pm 0.8 - (215$

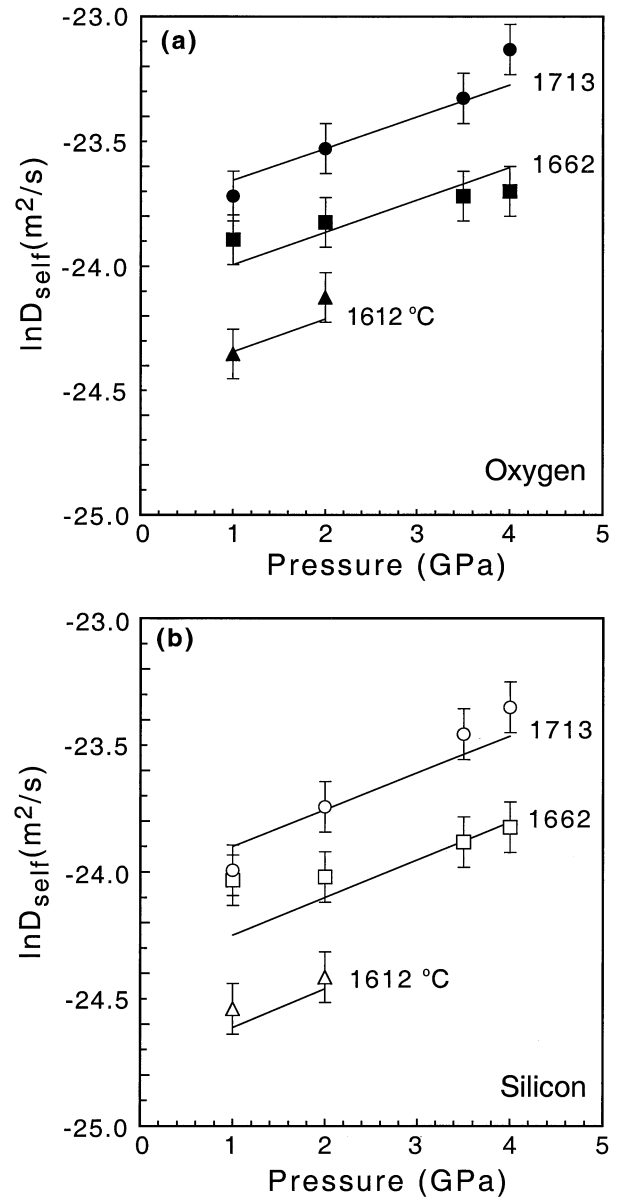


Fig. 4. (a) Pressure dependence of $\ln D(O)$. Data are plotted with 10% error bars on $D(O)$, determined by the reproducibility of multiple transects with ion microprobe. Between 1 and 4 GPa, these data obey the Arrhenius relationship $\ln D = \ln D_0 - (E_a + P\Delta V_a)/RT$. Multiple linear regression gives $\Delta V_a = -2.1 \pm 0.4$ cm³/mol for O self-diffusion. (b) Pressure dependence of $\ln D(Si)$. As in (a), data are plotted with 10% error bars on $D(Si)$. Between 1 and 4 GPa, these data obey the Arrhenius relationship listed in part (a). The data are plotted with best fit lines from multiple linear regression, which yields $\Delta V_a = -2.3 \pm 0.4$ cm³/mol for Si self-diffusion.

± 13 kJ/mol + $P(-2.1 \pm 0.4$ cm³/mol)/ RT , and the relationship for Si is $\ln D = -10.3 \pm 0.8 - (227 \pm 13$ kJ/mol + $P(-2.3 \pm 0.4$ cm³/mol)/ RT . These results are summarized in Table 3. The uncertainties in activation energy and activation volume in these relationships were determined using a Monte Carlo approach in the regression calculations. Regression coefficients were recalculated 1200 times, incorporating maxi-

Table 3. Regression coefficients from multiple linear regression for $\text{Di}_{58}\text{An}_{42}$.

Composition	NBO/T	Oxygen			Silicon		
		ΔV_a (cm^3/mol)	E_a (kJ/mol)	$\ln D_0$	ΔV_a (cm^3/mol)	E_a (kJ/mol)	$\ln D_0$
$\text{Di}_{58}\text{An}_{42}$	0.8	-2.1 ± 0.4	215 ± 13	-10.8 ± 0.8	-2.3 ± 0.4	227 ± 13	-10.3 ± 0.8
Basalt ^a	0.9	-8.1 ± 1.8	179 ± 13	-12.5 ± 0.9	-7.9 ± 3.2	174 ± 24	-12.9 ± 1.6
Dacite ^b	0.1	-9.2 ± 0.7	223 ± 29	-13.9 ± 1.9	-8.9 ± 0.7	200 ± 28	-15.8 ± 1.8

(a) Data from Lesher et al (1996).

(b) Data for 1-4 GPa and 1561 and 1662°C from Tinker and Lesher (2001).

um errors of $\pm 10\%$ on P/T , ± 0.000004 on $1/T$, and $\pm 10\%$ on $D(\text{O})$ and $D(\text{Si})$.

The activation energies for Si and O self-diffusion are similar to activation energies reported in recent experimental and MD simulation studies on other partially to fully polymerized liquid compositions (see Table 4). The absolute magnitudes of activation volumes in this study are among the smallest in the literature. For comparison, Table 5 shows activation volumes from the recent literature.

4. DISCUSSION

In summary, our experimental results show that Si and O self-diffusion coefficients increase with increases in pressure from 1 to 4 GPa and with increases in temperature from 1510 to 1764°C. The activation volumes are roughly $-2 \text{ cm}^3/\text{mol}$ for both Si and O self-diffusion. The activation energies for Si and O are also similar and are roughly 220 kJ/mol. The self-diffusion coefficients for O are slightly greater than those for Si, although this difference is within error for nearly all experiments.

4.1. Self-Diffusion Mechanism

The positive pressure dependence of Si and O self-diffusion can be explained by the formation and disassociation of five-coordinated Si (e.g., Liu et al., 1988; Farnan and Stebbins, 1994) or Al (Poe et al., 1997) intermediate species. Five-

coordinated Si has been inferred from NMR spectra of $\text{K}_2\text{Si}_4\text{O}_9$ glass cooled at various rates from 1300°C at atmospheric pressure (Stebbins, 1991), and five- and six-coordinated Si have been inferred from NMR spectra of $\text{K}_2\text{Si}_4\text{O}_6$ glass quenched from 1.9 GPa (Stebbins and McMillan, 1989). Increasing proportions of high-coordinated Al have been inferred from NMR spectra of $\text{Na}_3\text{AlSi}_7\text{O}_{17}$ quenched from pressures between 6 and 12 GPa, with the abundance of six-coordinated Al increasing continuously and the abundance of five-coordinated Al reaching a maximum at 8 GPa (Yarger et al., 1995). The self-diffusion of Si and O by the formation of high-coordinated Si or Al results in negative activation volumes with absolute magnitudes that are close to the molar volume of O ($6.9 \text{ cm}^3/\text{mol}$). Additional expectations for this type of ion exchange include similar Si and O self-diffusion coefficients and similar activation energies for Si and O self-diffusion. The new results for Si and O self-diffusion in $\text{Di}_{58}\text{An}_{42}$ liquid are consistent with these expectations, although the absolute magnitudes of the activation volumes are slightly smaller than the molar volume of O.

When no more five-coordinated Si or Al can form, self-diffusion coefficients reach maximum values. Angell et al. (1982) predicted a maximum O self-diffusion coefficient in $\text{NaAlSi}_2\text{O}_6$ liquid near 30 GPa, where the population of five-coordinated Si reached its maximum. More recently, Nevins and Spera (1998) predicted a maximum self-diffusion coefficient for O, and a maximum population of five-coordinated Si

Table 4. Activation energies for Si and O self diffusion in selected silicate liquid compositions.

Composition	NBO/T	P (GPa)	Oxygen	Silicon	Reference
			E_a (kJ/mol)	E_a (kJ/mol)	
Dacite	0.1	1	293 ± 10	380 ± 21	Tinker and Lesher (2001)
Dacite	0.1	2	264 ± 13	305 ± 28	Tinker and Lesher (2001)
Dacite	0.1	4	155 ± 14	163 ± 35	Tinker and Lesher (2001)
$\text{Di}_{60}\text{Jd}_{40}$	1	1		209	Shimizu and Kushiro (1991)
$\text{Di}_{60}\text{Jd}_{40}$	1	2		259	Shimizu and Kushiro (1991)
$\text{Di}_{20}\text{Jd}_{80}$	0.3	1		280	Shimizu and Kushiro (1991)
$\text{Di}_{20}\text{Jd}_{80}$	0.3	2		310	Shimizu and Kushiro (1991)

Table 5. Activation volumes for Si and O self diffusion in selected silicate liquid compositions.

Composition	NBO/T	T (°C)	P (GPa)	Oxygen	Silicon	Reference
				ΔV_a (cm ³ /mol)	ΔV_a (cm ³ /mol)	
Na ₂ Si ₄ O ₉	0.5		10–15	–2.8	–2.2	Poe et al. (1997)
Na ₂ Si ₄ O ₉	0.5		2.5–10	–3.3		Rubie et al. (1993)
Jadeite	0		0.5–2	–6.3		Shimizu and Kushiro (1984)
Diopside	2		1–1.7	8.48		Shimizu and Kushiro (1984)
Na ₃ AlSi ₇ O ₁₇	0.25		4–8	–5.4		Poe et al. (1997)
NaAlSi ₃ O ₈	0		2.5–4	–8.3		Poe et al. (1997)
Dacite	0.1	1460	1–4	–14.5	–17.1 ± 1.9	Tinker and Lesher (2001)
Dacite	0.1	1561	1–4	–9.8	–8.7 ± 1.4	Tinker and Lesher (2001)
Dacite	0.1	1662	1–4	–8.8	–9.3 ± 1.5	Tinker and Lesher (2001)
Jadeite ^a	0	3723	1–15	–5.9	–6.1	Bryce et al (1999)
NaAlSi ₃ O ₈ ^a	0	3723	1–15	–7.7	–7.7	Bryce et al (1999)

(a) Molecular dynamics simulation study.

and Al, at 5 GPa in CaAl₂Si₂O₈. Similarly, Bryce et al. (1999) predicted that maximum self-diffusion coefficients for Si, O, and Al coincide with maximum abundances of five-coordinated Si and Al in NaAlO₂-SiO₂ liquids at 21 GPa.

4.2. Compositional Dependence of Activation Volume

Previous workers have compared the self-diffusion of Si and O in silicate liquids to the degree of polymerization of the liquids. The best example of such a comparison is reproduced in Figure 1, which shows changes in the activation volumes for Si in Di-Jd liquids (Shimizu and Kushiro, 1991) with variations in NBO/T. As discussed earlier, Shimizu and Kushiro (1991) report that the transition from negative to positive activation volume in Di-Jd liquids occurs at NBO/T = 0.445. For comparison, we plot activation volumes for Si in Di₅₈An₄₂ liquid (NBO/T = 0.8), for Si in dacitic liquid (NBO/T = 0.1) at 1561°C (–8.7 cm³/mol), and for Si in basaltic liquid (NBO/T = 0.9) between 1320 and 1600°C (–7.9 cm³/mol) (Lesher et al., 1996; Tinker and Lesher, 2001). Two activation volumes for Si self-diffusion in Di are plotted in Figure 1. The activation volume of 2 cm³/mol, for pressures between 0.5 and 1.7 GPa at 1650°C, is from the piston cylinder experimental study of Shimizu and Kushiro (1991). The activation volume of 2.9 cm³/mol, for pressures between 3 and 6 GPa at 2000°C, is from the recent multianvil study of Reid et al. (2001). Interpolation between these activation volumes for endmember Di and the activation volume for Si in Di₅₈An₄₂ (–2.1 cm³/mol) gives a range of NBO/T between 1.2 and 1.4 for the transition from negative to positive activation volume in Di-An liquids. The differences in the NBO/T values predicted for transitions in pressure dependence, along with the observation that the activation volume for Si self-diffusion in basaltic liquid lies well off the trends defined by the data for Di-Jd and Di-An liquids, suggest that there are liquid structural controls on Si self-diffusion behavior that are not described well by the NBO/T index. Shimizu and Kushiro (1991) proposed that the pressure effect on self-diffusion behavior of compositions along the Di-Jd join is caused by changes in melt subsystems, similar to the terminology of Adam and Gibbs (1965) who equated “subsystems” and “cooperatively rearranging regions” when they described the structural relaxation of liquids. Cooperatively

rearranging regions can change their configurations independently of their surrounding environments. The existence of the subsystems envisioned by Shimizu and Kushiro (1991) accounts for configurational entropy that enhances self-diffusion of Si in intermediate compositions along the Di-Jd join.

There are no systematic studies of O self-diffusion along a compositional join, as are available for Si. However, there is an inverse relationship between the melt viscosity (η) and the O self-diffusion coefficient ($D(O)$) (e.g., in the Eyring equation $\eta = kT/D(O)\lambda$, where k is the Boltzmann constant and λ is the characteristic jump distance for diffusion), which allows a comparison of the pressure dependence of melt viscosity and the pressure dependence of self-diffusion. The Eyring equation successfully predicts the sense of the pressure dependence of viscosities of depolymerized liquids such as Di (e.g., Shimizu and Kushiro, 1984; Reid et al., 2001), although it is unable to predict their magnitudes accurately. Kushiro (1981) found a transition from negative to positive pressure dependence of viscosity near the anorthite composition in the CaAl₂O₄-SiO₂ system in which all liquids have NBO/T = 0, while Brearley et al. (1986) found a viscosity minimum for Ab₂₅Di₇₅ liquid (NBO/T = 1.2) at roughly 1.2 GPa. For the Di-An system, the negative activation volume we determined for Di₅₈An₄₂ melt (e.g., –2.1 cm³/mol) coupled with values for pure Di melts between 8.48 cm³/mol (Shimizu and Kushiro, 1984) and 3 cm³/mol (Reid et al., 2001) predicts by linear interpolation that the activation volume will be zero at an NBO/T between 1 and 1.3. Although this range brackets the NBO/T reported by Brearley et al. (1986) for the change in the sign of ΔV_a in the Di-Ab system, it is clear from Kushiro’s (1981) work on fully polymerized melts that NBO/T alone is not a reliable index for the sign of the activation volume. In the next section, we show how Adam-Gibbs theory (Adam and Gibbs, 1965) can be used to unify the results for polymerized and depolymerized melts.

4.3. Adam-Gibbs Theory

A relationship between melt viscosity and configurational entropy is derived from the probability of structural rearrangement of a liquid (Adam and Gibbs, 1965). The Adam-Gibbs theory results in an inverse relationship between the natural log of the viscosity (η) and configurational entropy (S_{conf}): $\ln \eta =$

$A_e + B_e/TS_{\text{conf}}$, where A_e and B_e are constants that depend mainly on composition (e.g., Richet, 1984). This relationship has been applied to viscosities of silicate liquids near the glass transition (e.g., Bottinga et al., 1995; Bottinga and Richet, 1996; Toplis, 1998, 2001).

Bottinga and Richet (1995) modified the Adam-Gibbs theory to explain experimental results showing that viscosities of polymerized liquids decrease with pressure and viscosities of depolymerized liquids increase with pressure. They derived:

$$\left[\frac{\partial \ln(\eta)}{\partial P} \right]_T = \frac{B_e}{TS_{\text{conf}}^2} \left[\left[\frac{\partial V_{\text{conf}}}{\partial T} \right]_P + \left[\frac{\partial \xi}{\partial P} \right]_T \text{RN}_0 \ln \left(\frac{\xi}{1-\xi} \right) \right] \quad (3)$$

where V_{conf} (defined as $V_{\text{liquid}} - V_{\text{glass}}$) is the configurational volume, N_0 is the number of O atoms divided by the number of simple oxide moles per formula unit (e.g., $N_0 = 2$ for $\text{NaAlSi}_2\text{O}_6$ and $N_0 = 1.5$ for $\text{CaMgSi}_2\text{O}_6$), and ξ is the fraction of bridging oxygen (BO) in the melt ($\xi = \text{BO}/\text{total O}$). The critical term in Eqn. 3 is $\ln[\xi/(1-\xi)]$, which is positive in polymerized liquids (where $\xi > 0.5$) and negative in depolymerized liquids (where $\xi < 0.5$). The change in sign with composition of this term is important, because the signs of the other terms in Eqn. 3 are constant for silicate liquids. First, B_e and S_{conf} are positive, so (B_e/TS_{conf}^2) is positive. Second, because the coefficients of thermal expansion for silicate liquids are in general greater than those for the corresponding glasses (Lange, 1997), $(\partial V_{\text{conf}}/\partial T)_P$ is positive for silicate liquids. Third, $(\partial \xi/\partial P)_T$ is negative in silicate liquids because the partial molar volume of bridging oxygens is greater than the partial molar volume of nonbridging oxygens (Bottinga and Richet, 1995). Therefore, if the magnitude of the $(\partial V_{\text{conf}}/\partial T)_P$ term is sufficiently small, the positive $\ln[\xi/(1-\xi)]$ in polymerized liquids gives a negative pressure dependence of viscosity, and the negative $\ln[\xi/(1-\xi)]$ in depolymerized liquids gives a positive pressure dependence of viscosity.

Recently, Bryce et al. (1999) extended the Adam-Gibbs theory to describe the pressure dependence of $D(\text{O})$. These authors assumed that because of the inverse relationship between η and $D(\text{O})$, $(\partial \ln \eta / \partial P)_T = -[(\partial \ln D(\text{O})) / \partial P]_T$. Substitution into Eqn. 3 gives:

$$\left[\frac{\partial \ln(D(\text{O}))}{\partial P} \right]_T = - \frac{B_e}{TS_{\text{conf}}^2} \left[\left[\frac{\partial V_{\text{conf}}}{\partial T} \right]_P + \left[\frac{\partial \xi}{\partial P} \right]_T \text{RN}_0 \ln \left(\frac{\xi}{1-\xi} \right) \right] \quad (4)$$

Further, the Arrhenius relationship $D = D_0 \exp(-P\Delta V_a/RT)$ gives $\Delta V_a = -RT[(\partial \ln D(\text{O})) / \partial P]_T$, and substitution into Eqn. 4 yields:

$$\Delta V_a = \frac{RB_e}{S_{\text{conf}}^2} \left[\left[\frac{\partial V_{\text{conf}}}{\partial T} \right]_P + \left[\frac{\partial \xi}{\partial P} \right]_T \text{RN}_0 \ln \left(\frac{\xi}{1-\xi} \right) \right] \quad (5)$$

Eqn. 5 has the same form as the equation derived by Bryce et al. (1999) (see their Eqn. 3). The only difference is that they substituted $\psi = {}^{12}\text{O}/({}^{12}\text{O} + {}^{13}\text{O})$ for ξ in Eqn. 5, because they predicted that O in $\text{NaAlO}_2\text{-SiO}_2$ liquids exist mainly as two-coordinated (${}^{12}\text{O}$) and three-coordinated (${}^{13}\text{O}$) species. Bryce et al. (1999) found good agreement between the predicted

pressure of maximum Si, O, and Al self-diffusion coefficients and the predicted pressure, where $\psi = 0.5$ (${}^{12}\text{O} \approx {}^{13}\text{O}$).

4.4. Oxygen-Bonding Controls on Self-Diffusion

In this section, we examine the relationship between ξ and ΔV_a for O self-diffusion in polymerized and depolymerized silicate liquid compositions. The application of Adam-Gibbs theory depends on the parameters used in Eqn. 5 (see Table 6 for parameters used here). To determine the parameters in Eqn. 5, we make two important simplifications. First, we substitute dV/dT for $(\partial V_{\text{conf}}/\partial T)_P$, and we use molar oxide contributions from Lange (1997) to estimate dV/dT for liquids along the Di-An join. This substitution is justified because the thermal expansion of most silicate liquids is more than an order of magnitude greater than the thermal expansion of the same composition of silicate glass (e.g., Lange, 1997). Second, we treat $\partial \xi/\partial P$ as a constant independent of $\ln[\xi/(1-\xi)]$. Although this is an oversimplification of the behavior of silicate liquids, this approach allows us to constrain ξ uniquely for a given liquid composition and ΔV_a .

In our initial calculations, we assign ξ for Di and An liquids. We use $\xi = 0.33$ for Di, based on the stoichiometry (Bottinga and Richet, 1995), and we use $\xi = 0.95$ for An, based on MD simulations (5% NBO at $P < 5$ GPa; Nevins and Spera, 1998). The B_e values for Di and An are from Richet (1984). We calculate S_{conf} following Richet et al. (1986), using configurational entropy and heat capacity terms from Richet (1984). For Di, we use $\Delta V_a = 8.48 \text{ cm}^3/\text{mol}$ as reported by Shimizu and Kushiro (1984), because this piston cylinder study presents the lowest pressure experimental results available in the literature. For An, we use $\Delta V_a = -3 \text{ cm}^3/\text{mol}$, from MD simulations for 2 to 5 GPa (Nevins and Spera, 1998). Finally, we calculate $\partial \xi/\partial P$ for Di and An using Eqn. 5.

The parameters for $\text{Di}_{58}\text{An}_{42}$ liquid in Eqn. 5 are determined by interpolating linearly between Di and An. We use contributions of endmember values in molar proportions (i.e., 36% of the An value summed with 64% of the Di value) to estimate S_{conf} and B_e for $\text{Di}_{58}\text{An}_{42}$ liquid. To determine ξ for $\text{Di}_{58}\text{An}_{42}$, we interpolate (with step sizes of 0.002) between ξ values for Di and An, and we calculate dV/dT (in increments of 2 mol.%) for intermediate Di-An compositions (Lange, 1997). The value $\xi = 0.84$ for $\text{Di}_{58}\text{An}_{42}$ is at the same incremental step between endmembers as dV/dT calculated for $\text{Di}_{58}\text{An}_{42}$. We use this correlation because dV/dT can be determined reliably for silicate liquids. As we did for Di and An, we calculate the value of $\partial \xi/\partial P$ for $\text{Di}_{58}\text{An}_{42}$.

Figure 5a shows the changes in ξ and ΔV_a with increasing Di content in the liquid. The ΔV_a values for O self-diffusion in Di from Shimizu and Kushiro (1984) and Reid et al. (2001) are included in this plot to show the possible range of ΔV_a at low to moderate pressures. The most important feature of Figure 5a is that An and $\text{Di}_{58}\text{An}_{42}$ have similar ξ values, and these values are much greater than ξ for Di. The sharp decrease in ξ between $\text{Di}_{58}\text{An}_{42}$ and Di coincides with a transition from negative to positive ΔV_a . Interpolating between the two ΔV_a values for Di and the ΔV_a for $\text{Di}_{58}\text{An}_{42}$, we predict that the transition from positive to negative pressure dependence will occur in liquid compositions with 65 to 75 wt.% Di. These liquids have ξ between 0.62 and 0.73. In other words, the Adam-Gibbs theory

Table 6. Parameters used in Eqn. 5. The values of ξ for Di and An at low pressure are estimated from stoichiometry (Bottinga and Richet, 1995), and ξ for Ab, Jd, and $\text{Di}_{58}\text{An}_{42}$ at low pressure are from interpolations between Di and An endmembers (see text). The value of $(\partial\xi/\partial P)_T$ is calculated based on other parameters, and N_0 is from stoichiometry. The values of ξ for Di and Ab at high pressures are necessary to reproduce ΔV_a in Eqn. 5, keeping all other parameters constant.

Liquid composition	ΔV_a (cm^3/mol)	$S_{\text{conf}}^{\#}$	B_e ($\times 10^{-5}$) [†]	$(\partial V/\partial T)_P$ ($\times 10^3$) [¥]	$(\partial\xi/\partial P)_T$ ($\times 10^5$)	N_0	ξ
$\text{Di}_{58}\text{An}_{42}$	-2.1 ^a	84.39	4.66	1.41	-2.4	1.71	0.84
Diopside	8.48 ^b	80.16	3.96	1.75	-17	1.5	0.33
Diopside (3-6 GPa)	3 ^c	93.81	3.96	1.75	-17	1.5	0.43
Diopside (11-13 GPa)	-6.7 ^c	93.81	3.96	1.75	-17	1.5	0.72
Jadeite	-6.3 ^b	42.03	3.12	1.28	-1.4	2	0.91
Jadeite	-5.9 ^d	42.03	3.12	1.28	-1.4	2	0.90
Anorthite	-3 ^e	91.90	5.63	0.94	-1.3	2	0.95
Albite	-7.7 ^d	81.01	5.64	0.96	-2.6	2	0.94
Albite (2.5-4 GPa)	-8.3 ^f	81.01	5.64	0.96	-2.6	2	0.95
Albite (4-5 GPa)	-0.9 ^g	81.01	5.64	0.96	-2.6	2	0.63
Albite (5-6 GPa)	0.9 ^g	81.01	5.64	0.96	-2.6	2	0.48

(#) Calculated following Richet et al. (1986).

(†) From Richet (1984).

(¥) Calculated following Lange (1997).

(a) This study.

(b) Shimizu and Kushiro (1984).

(c) Reid et al. (2001).

(d) Bryce et al. (1999).

(e) Nevins and Spera (1998).

(f) Poe et al. (1997).

(g) Estimated for 4-5 GPa and 5-6 GPa from Poe et al. (1997).

predicts that the transition from positive to negative ΔV_a will occur when 62 to 73% of oxygen in a Di-An liquid is bridging oxygen.

The Adam-Gibbs analysis can also be used to explore the relationship between ξ and ΔV_a for Jd and Ab liquids in addition to Di-An liquids. This analysis evaluates changes in liquid structure due to compression of a constant liquid composition. Low pressure values of ΔV_a for O self-diffusion are those values reported in the literature for the lowest pressure ranges available. The ξ for Jd and Ab liquids at low pressure are determined by interpolation between 0.33 (Di) and 0.95 (An). We choose values for ξ that correspond to dV/dT calculated for Jd and Ab. The parameters for S_{conf} and B_e for Jd and Ab are from Richet (1984), and we calculate $\partial\xi/\partial P$ using Eqn. 5. We estimate ΔV_a for O self-diffusion at high pressures using O self-diffusion coefficients in Ab from 4 to 6 GPa (Poe et al., 1997) and Di from 3 to 6 GPa and 11 to 13 GPa (Reid et al., 2001). We allow only ξ and ΔV_a to change with pressure. The change in liquid structure with pressure is measured by the change in ξ necessary to reproduce ΔV_a using Eqn. 5. Table 6 shows a list of all parameters used in Eqn. 5.

Figure 5b shows the ξ - ΔV_a relationship for Di and Ab liquids with increasing pressure, the ξ - ΔV_a relationship for liquid compositions along the Di-An join, and the ξ - ΔV_a relationship for Jd liquid. There is a general trend of decreasing ΔV_a with increasing ξ , and we use this trend to make a prediction of the pressure dependence of O self-diffusion in silicate liquids. The line running through the data is a least-squares-best-fit to all of the data. This line crosses $\Delta V_a = 0$ at $\xi \approx 0.6$. Therefore, we expect transitions from positive to negative ΔV_a for O self-diffusion when 60% of oxygen is bridging oxygen. This estimate is not precise because of scatter in the data. However, this scatter may be due to differences in diffusion mechanisms as O self-diffusion passes through a minimum or a maximum. For

example, the ξ - ΔV_a relationship for depolymerized Di, in which O self-diffusion coefficients pass through a minimum, has a steep, negative trend. In contrast, a shallower trend is defined by the ξ - ΔV_a relationship for polymerized Ab, in which O self-diffusion coefficients pass through a maximum. To understand the differences in these ξ - ΔV_a relationships, more experimental work must be performed to determine the pressure dependence of O self-diffusion in depolymerized liquid compositions.

5. CONCLUSIONS

This study shows that the Adam-Gibbs theory is useful for understanding the relationship between melt structure (ξ) and activation volume for O self-diffusion. The new self-diffusion data for $\text{Di}_{58}\text{An}_{42}$ liquid in this study allow a comparison of ξ and ΔV_a for liquids along the Di-An join. The Adam-Gibbs analysis emphasizes similarities between transitions from positive to negative activation volume that are due to changes in liquid composition and the transitions from positive to negative activation volume that occur when liquids of constant composition are compressed. Both compositionally driven and pressure-induced transitions reflect silicate liquid structures with ξ of 0.6 to 0.65. Similarities in the structures of liquids undergoing transitions from positive to negative activation volume are important experimentally. Detailed experimental and spectroscopic studies of silicate liquid compositions that have small activation volumes at low pressures may provide important information on the liquid structure controlling the dynamic behavior of liquids such as Ab and Di in which maximum and minimum self-diffusion coefficients have been observed at high pressures. Understanding these simple systems will further elucidate the properties of naturally occurring silicate melts at high pressures.

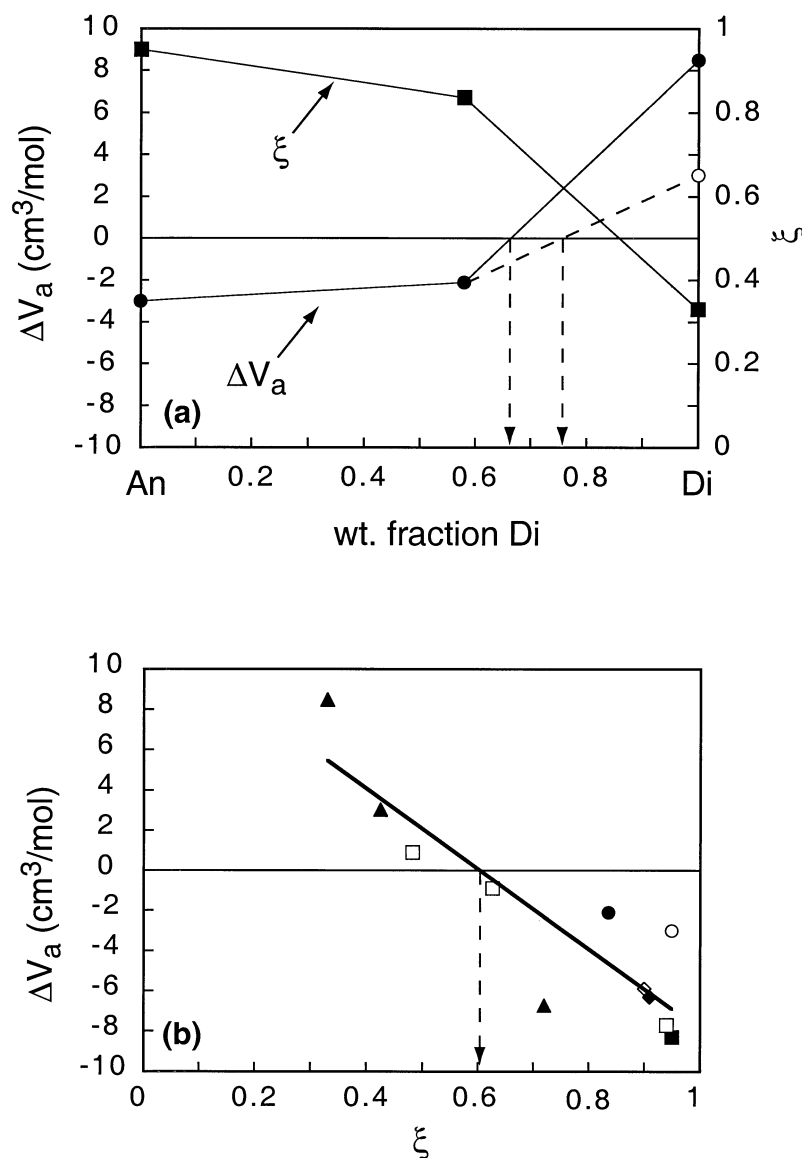


Fig. 5. (a) Variation of activation volume (ΔV_a) for O self-diffusion (circles) and variation of ξ (squares) with change in composition along the Di-An join (wt. fraction Di). The activation volume of $-3 \text{ cm}^3/\text{mol}$ for An liquid is estimated from MD predictions of Nevins and Spera (1998), and the activation volume of $-2.1 \text{ cm}^3/\text{mol}$ for $\text{Di}_{58}\text{An}_{42}$ liquid is from multiple linear regressions on O self-diffusion coefficients in this study (see Table 3). The activation volumes for Di are taken from Shimizu and Kushiro (1984) ($8.48 \text{ cm}^3/\text{mol}$) and from Reid et al. (2001) ($3.0 \text{ cm}^3/\text{mol}$). Interpolation between these data suggests that the transition from positive to negative activation volume in the Di-An system occurs between $\text{Di}_{65}\text{An}_{35}$ and $\text{Di}_{75}\text{An}_{25}$. These compositions correspond to ξ between 0.62 and 0.73. (b) Correlation of ΔV_a for O self-diffusion with ξ is calculated using Eqn. 5 (see text). The ΔV_a for Di (triangles) are from Shimizu and Kushiro (1984) ($8.48 \text{ cm}^3/\text{mol}$, 1–1.7 GPa) and Reid et al. (2001) ($3.0 \text{ cm}^3/\text{mol}$, 3–6 GPa; $-6.7 \text{ cm}^3/\text{mol}$, 11–13 GPa). The ΔV_a for Ab (squares) are from Bryce et al. (1999) ($-7.7 \text{ cm}^3/\text{mol}$, open square) and Poe et al. (1997) for 2.5 to 4 GPa ($-8.3 \text{ cm}^3/\text{mol}$, filled square). The ΔV_a for Ab from 4 to 5 GPa ($-0.9 \text{ cm}^3/\text{mol}$, open square) and from 5 to 6 GPa ($0.9 \text{ cm}^3/\text{mol}$, open square) are calculated using data from Poe et al. (1997). Additional ΔV_a include Jd ($-6.3 \text{ cm}^3/\text{mol}$, filled diamond) between 0.5 and 2 GPa (Shimizu and Kushiro, 1984), Jd ($-5.9 \text{ cm}^3/\text{mol}$, open diamond) to 21 GPa (Bryce et al., 1999), An ($-3 \text{ cm}^3/\text{mol}$, open circle) between 2 and 5 GPa (Nevins and Spera, 1998), and $\text{Di}_{58}\text{An}_{42}$ ($-2.1 \text{ cm}^3/\text{mol}$, filled circle). A best fit line to these data shows a transition from positive to negative activation volume at $\xi \approx 0.6$.

Acknowledgments—The authors thank F. J. Spera and an anonymous reviewer for comments that improved the manuscript. Editorial handling and additional helpful comments from R. Ryerson are also acknowledged. Work was performed under the auspices of the U.S. Department of Energy by Lawrence Livermore National Laboratory under Contract W-7405-ENG-48. This work was supported by IGPP GS96-33 (CEL) and EAR-00-01245 (CEL).

Associate editor: F. J. Ryerson

REFERENCES

- Adam G. and Gibbs J. H. (1965) On the temperature dependence of cooperative relaxation properties in glass-forming liquids. *J. Chem. Phys.* **43**, 139–146.

- Angell C. A., Cheeseman P. A., and Tamaddon S. (1982) Pressure enhancement of ion mobilities in liquid silicates from computer simulation studies to 800 kilobars. *Science* **218**, 885–887.
- Bottinga Y. and Richet P. (1995) Silicate melts: The “anomalous” pressure dependence of the viscosity. *Geochim. Cosmochim. Acta* **59**, 2725–2731.
- Bottinga Y. and Richet P. (1996) Silicate melt structural relaxation: Rheology, kinetics, and Adam-Gibbs theory. *Chem. Geol.* **128**, 129–141.
- Bretherton M., Dickinson J. E. Jr, and Scarfe C. M. (1986) Viscosity regimes of homogeneous silicate melts. *Am. Mineral.* **80**, 305–318.
- Boyd F. R. and England J. L. (1960) Apparatus for phase equilibrium measurements at pressures up to 50 kilobars and temperatures up to 1750° C. *J. Geophys. Res.* **65**, 741–748.
- Bretherton M., Dickinson J. E. Jr, and Scarfe C. M. (1986) Pressure dependence of melt viscosities on the join diopside-albite. *Geochim. Cosmochim. Acta* **50**, 2563–2570.
- Bryce J. G., Spera F. J., and Stein D. J. (1999) Pressure dependence of self-diffusion in the NaAlO₂-SiO₂ system: Compositional effects and mechanisms. *Am. Mineral.* **84**, 345–356.
- Crank J. (1975) *The Mathematics of Diffusion*. Clarendon Press, Oxford.
- Dunn T. (1982) Oxygen diffusion in three silicate melts along the join diopside-anorthite. *Geochim. Cosmochim. Acta* **47**, 2292–2299.
- Farnan I. and Stebbins J. F. (1994) The nature of the glass transition in a silica-rich oxide melt. *Science* **265**, 1206–1209.
- Kushiro I. (1981) Change in viscosity with pressure of melts in the system CaO-Al₂O₃-SiO₂. *Carnegie Institution of Washington Yearbook*. **80**, 339–341.
- Lange R. A. (1997) A revised model for the density and thermal expansivity of K₂O-Na₂O-CaO-MgO-Al₂O₃-SiO₂ liquids from 700 to 1900 K: Extension to crustal magmatic temperatures. *Contrib. Mineral. Petrol.* **130**, 1–11.
- Lesher C. E., Hervig R. L., and Tinker D. (1996) Self diffusion of network formers (silicon and oxygen) in naturally occurring basaltic liquid. *Geochim. Cosmochim. Acta*. **60**, 405–413.
- Liu S.-B., Stebbins J. F., Schneider E., and Pines A. (1988) Diffusive motion in alkali silicate melts: An NMR study at high temperature. *Geochim. Cosmochim. Acta* **58**, 3653–3664.
- Mysen B. O. (1990) Relationships between silicate melt structure and petrologic processes. *Earth Sci. Rev.* **27**, 281–365.
- Nevins D. and Spera F. J. (1998) Molecular dynamics simulations of molten CaAl₂Si₂O₈: Dependence of structure and properties on pressure. *Am. Mineral.* **83**, 1220–1230.
- Poe B. T., McMillan P. F., Rubie D. C., Chakraborty S., Yarger J., and Diefenbacher J. (1997) Silicon and oxygen self-diffusivities in silicate liquids measured to 15 gigapascals and 2800 Kelvin. *Science* **276**, 1245–1248.
- Reid J. E., Poe B. T., Rubie D. C., Zotov N., and Wiedenback M. (2001) The self-diffusion of silicon and oxygen in diopside (CaMgSi₂O₆) liquid up to 15 GPa. *Chem. Geol.* **174**, 77–86.
- Richet P. (1984) Viscosity and configurational entropy of silicate melts. *Geochim. Cosmochim. Acta* **48**, 471–483.
- Richet P., Robie R. A., and Hemingway B. S. (1986) Low-temperature heat capacity of diopside glass (CaMgSi₂O₆): A calorimetric test of the configurational theory applied to the viscosity of liquid silicates. *Geochim. Cosmochim. Acta* **50**, 1521–1533.
- Rubie D. C., Ross C. R. II, Carroll M. R., and Elphick S. C. (1993) Oxygen self diffusion in Na₂Si₄O₉ liquid up to 10 GPa and estimation of high-pressure melt viscosities. *Am. Mineral.* **78**, 574–582.
- Scarfe C. M., Cronin D. J., Wenzel J. T., and Kauffman D. A. (1983) Viscosity-temperature relationships at 1 atm in the system diopside-anorthite. *Am. Mineral.* **68**, 1083–1088.
- Shimizu N. and Kushiro I. (1984) Diffusivity of oxygen in jadeite and diopside melts at high pressures. *Geochim. Cosmochim. Acta* **48**, 1295–1303.
- Shimizu N. and Kushiro I. (1991) The mobility of Mg, Ca, and Si in diopside-jadeite liquids at high pressures. In *Physical Chemistry of Magmas. Advances in Physical Geochemistry*, Vol. 9 (eds. L. L. Perchuk and I. Kushiro), pp. 192–212. Springer-Verlag, New York.
- Stebbins J. F. (1991) NMR evidence for five-coordinated silicon in a silicate glass at atmospheric pressure. *Nature* **351**, 638–639.
- Stebbins J. F. and McMillan P. (1989) Five- and six-coordinated Si in K₂Si₄O₉ glass quenched from 1.9 GPa and 1200°C. *Am. Mineral.* **74**, 965–968.
- Tinker D. and Lesher C. E. (2001) Self diffusion of Si and O in dacitic liquid at high pressures. *Am. Mineral.* **86**, 1–13.
- Toplis M. J. (1998) Energy barriers to viscous flow and the prediction of glass transition temperatures of molten silicates. *Am. Mineral.* **83**, 480–490.
- Toplis M. J. (2001) Quantitative links between microscopic properties and viscosity of liquids in the system SiO₂-Na₂O. *Chem. Geol.* **174**, 321–331.
- Walker D., Carpenter M. A., and Hitch C. M. (1990) Some simplifications to multi-anvil devices for high pressure experiments. *Am. Mineral.* **75**, 1020–1028.
- Yarger J. L., Smith K. H., Nieman R. A., Diefenbacher J., Wolf G. H., Poe B. T., and McMillan P. F. (1995) Al coordination changes in high-pressure aluminosilicate liquids. *Science* **270**, 1964–1967.